Electronic Supplementary Material (ESI) for Soft Matter

Lateral surface engineering of hybrid lipid/BCP vesicles and selective nanoparticle embedding

Matthias Schulz[a], *Adekunle Olubummo*[a], *Kirsten Bacia*[b] *and Wolfgang H. Binder*[a]*

[a] Martin-Luther University Halle-Wittenberg, Chair of Macromolecular Chemistry, Faculty of Natural Sciences II (Chemistry, Physics and Mathematics), Institute of Chemistry, D-06120 Halle (Saale), Germany.
[b] Martin-Luther University Halle-Wittenberg, ZIK HALOmem, D-06120 Halle(Saale), Germany.

Supplementary Information

Figures

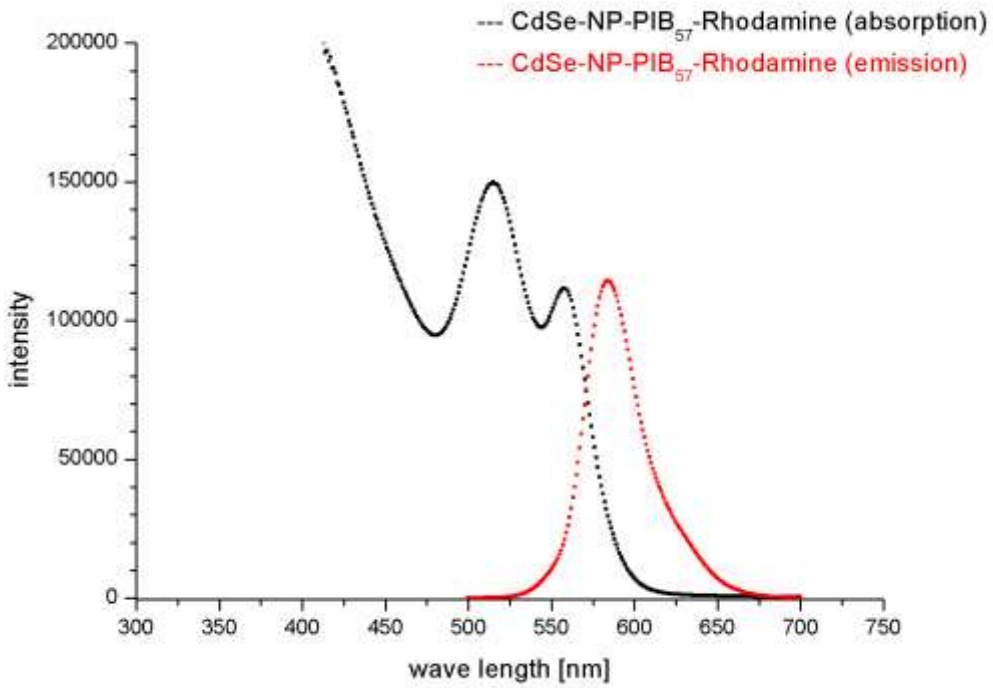

Figure S1. Absorption and emission spectra of hydrophobically modified CdSe nanoparticles, which are covalently labeled with rhodamine-B (excitation, λ_{max} = 561 nm).

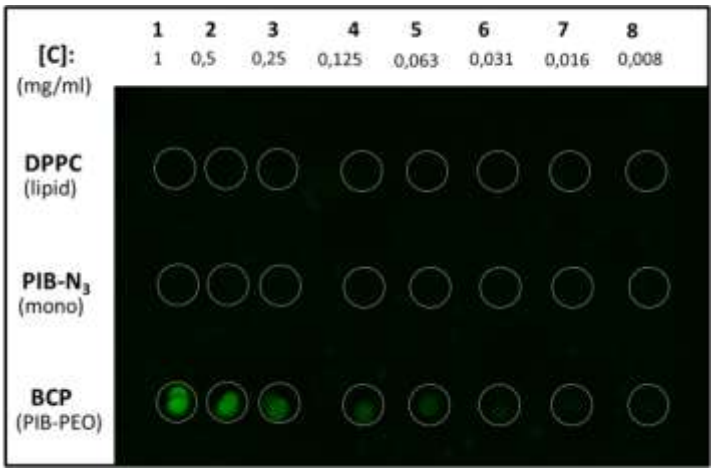

Figure S2. To examine the specificity of the antibody system against the PEO-functionality of PIB-PEO based block copolymers, we performed a dotblot experiment. Therefore, DPPC as lipid component, the PIB-homopolymer and the PIB_{87}-*b*-PEO_{17} BCP were blotted on a nitro-cellulose membrane varying their concentrations and subsequently the membrane was treated with a solution of dry milk to block unspecific interactions of antibodies with membrane. After 1 hour, the membrane was washed with buffer solution (three times) and then incubated with the primary antibody (anti-PEO). Afterwards (again 1 hour), the membrane was washed three times with buffer solution (a 20 min) and subsequently the membrane was incubated with the secondary antibody (anti-rabbit, fluorescently labeled with dylight 488 dye). Before the detection of the antibody by fluorescence analysis was carried out, the membrane was washed again three times with buffer solution and slightly dried. The fluorescence analysis (see green areas) is shown in Figure S2 demonstrating that the binding of the antibody system was only observed in case of the blotted BCP sample. DPPC or PIB-homopolymers were not detected by the antibodies confirming the high specificity of antibody system.

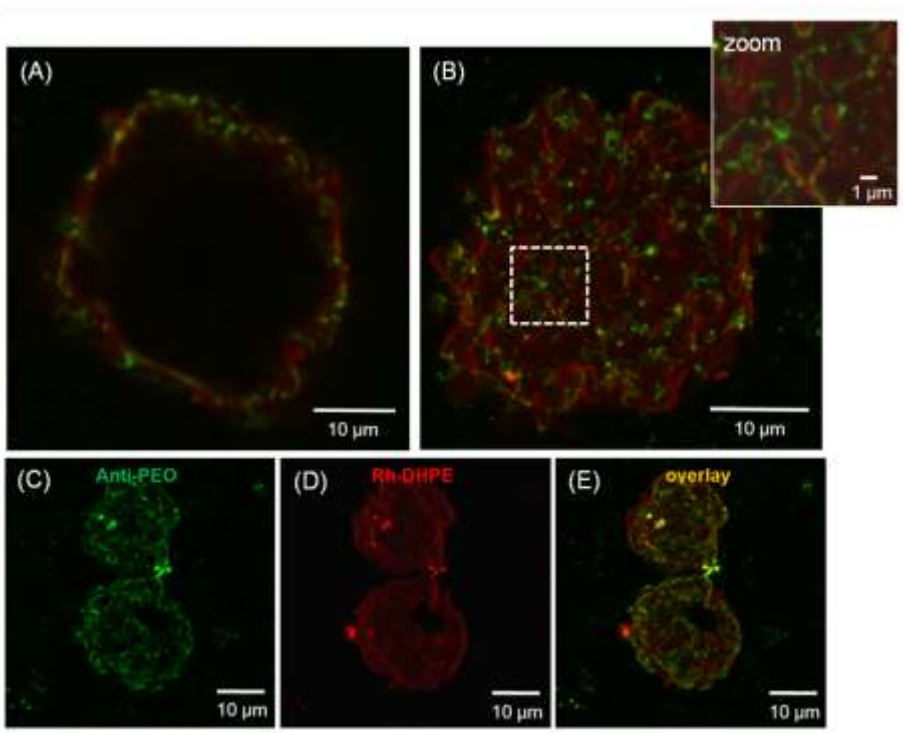

Figure S3. Confocal microscopy images of hybrid GUVs prepared from a mixture of DPPC with 10 mol% of BCP demonstrating that the binding of the antibodies to the incorporated BCPs revealed a network-like morphology of the BCPs within the facetted vesicle surface. Panel (A) depicts an image of a facetted hybrid vesicle, which is typical for such lipid/BCP composition, near the vesicle equator showing the binding of the antibodies to BCPs (green patches in A). (B) 3D-reconstruction of an axial series of confocal slices from the vesicle shown in (A), which proves the network-like morphology of the incorporated BCPs (see green areas in the zoom). Panel (C-E) displays a 3D-reconstruction of single

GUVs indicating the uniform distribution of the Rh-DHPE dye over the whole GUV surface (D) and the binding of the antibodies to BCP molecules proving finally heterogeneous distribution of the BCPs in the facetted vesicle surface.

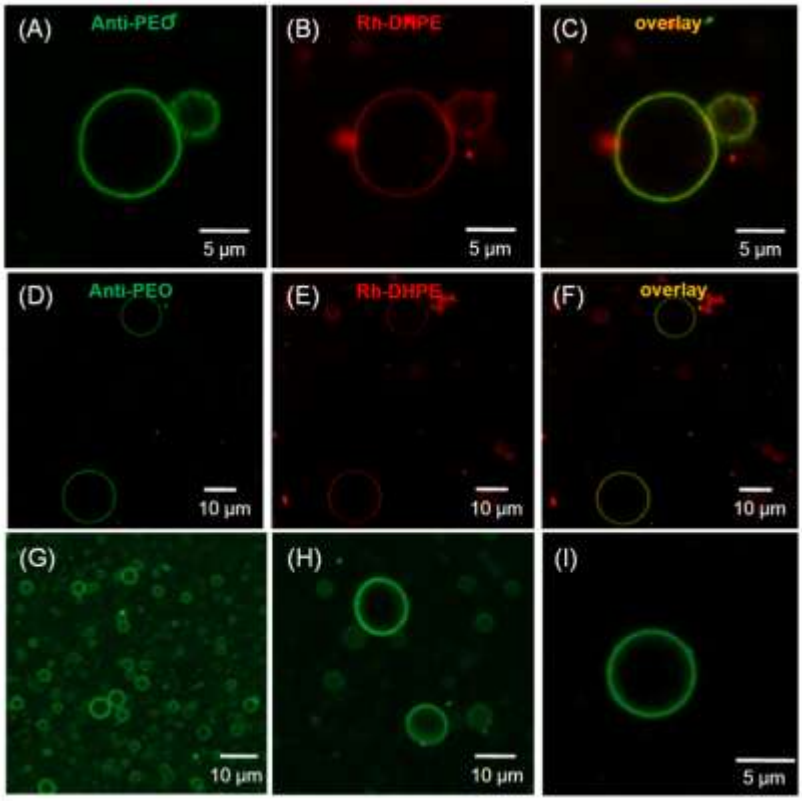

Figure S4. Confocal microscopy images of hybrid GUVs from DPPC mixed with 16 mol% of BCP showing in (A to C) a single vesicle typically obtained for such composition, which demonstrate a random distribution of the membrane components within the mixed bilayer by comparing the fluorescence signal of the antibody with fluorescence of Rh-DHPE dye. (D-F) illustrates an overview of single GUVs proving the mixed membrane morphology by the uniform fluorescence of both dyes. Panel (G to F) shows vesicles from another experiment visualizing the vesicles only by recognition of the membrane incorporated BCPs by antibodies (no additional membrane dye was used). The antibodies bind over the whole hybrid vesicle surface, which indicates that the polymers are randomly distributed in the membrane.

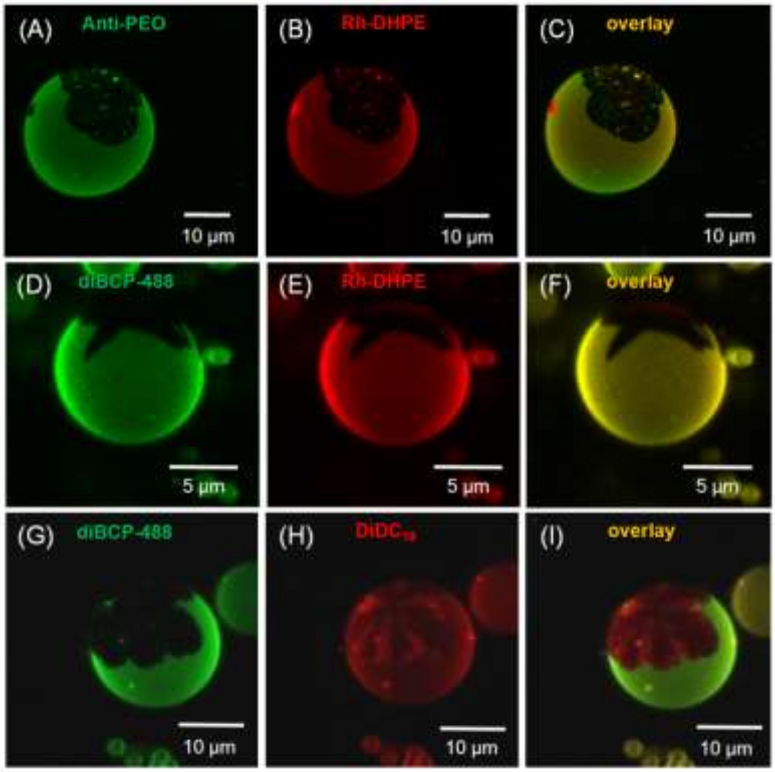

Figure S5. Confocal microscopy images of phase-separated hybrid DPPC/PIB_{87}-*b*-PEO_{17} GUVs obtained with 76 mol% DPPC and 24 mol% BCP, demonstrating membrane heterogeneities by the phase partitioning behavior of the lipid analogous $DiDC_{18}$ dye, rhodamine-labeled lipid (Rh-DHPE) and the fluorescently labeled PIB-PEO diblock copolymer (diBCP-488) in comparison to the results of the antibody-mediated monitoring of BCPs (A-C). The first row (panel A to C) shows a 3D- reconstruction of an axial series of confocal slices of a phase separated vesicle where the polymer-rich phase was successfully assigned by the antibody binding (compare panel A, green phase). Panel (D-F) depicts also a 3D-reconstruction of a phase separated GUV, where the polymer-rich phase was successfully assigned by using the fluorescently labeled diblock copolymer (excited at 488 nm, green phase in panel D). The use of Rh-DHPE proves that the membrane dye is preferential incorporated into the polymer-rich phase, as illustrated in panel B and E. Whereas, visualization of phase heterogeneities in hybrid GUVs (Panel G-F, 3D-reconstruction) by the lipid analogous dye $DiDC_{18}$ showed an enrichment of the dye in the black domain, as proved by the fluorescently labeled block copolymer or antibody binding to be the DPPC-rich phase (compare panel G with H), that this particular phase is formed by highly ordered DPPC molecules. In contrast to the reported phase partitioning behavior of Rh-DHPE,[1, 2] $DiDC_{18}$ has shown to become enriched into more ordered gel-phase domains in GUVs prepared from phospholipids, which differ in their acyl-chain lengths.[3]

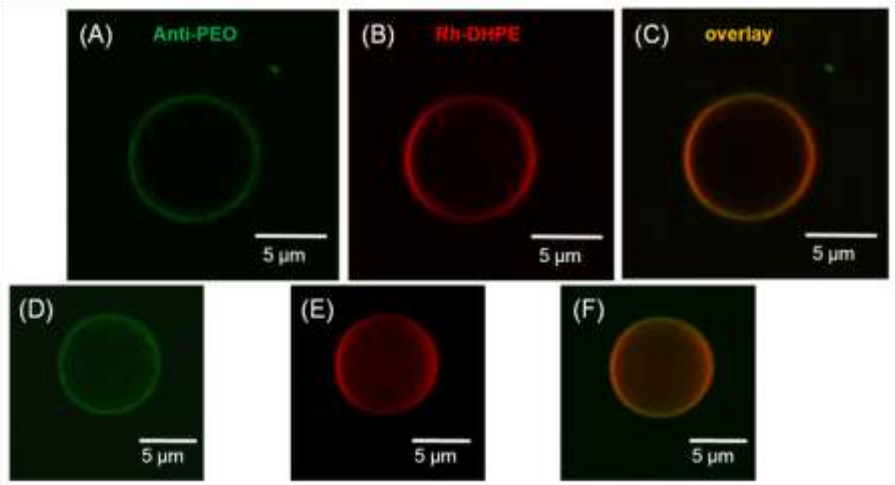

Figure S6. Confocal microscopy images of mixed hybrid DPPC/PIB_{87}-*b*-PEO_{17} GUVs obtained with 60 mol% DPPC and 40 mol% BCP proving the formation of the mixed phase by antibody-mediated monitoring of membrane incorporated BCP molecules (panel A and D). Panel (A to C) shows a single equatorial slice of a hybrid GUV and panel (D to F) depicts a 3D-reconstruction of an axial series of confocal slice from a vesicle, which is typically obtained for 60/40 mixtures of DPPC and BCP demonstrating a uniform distribution of the antibodies and the Rh-DHPE dye over the whole GUV membrane.

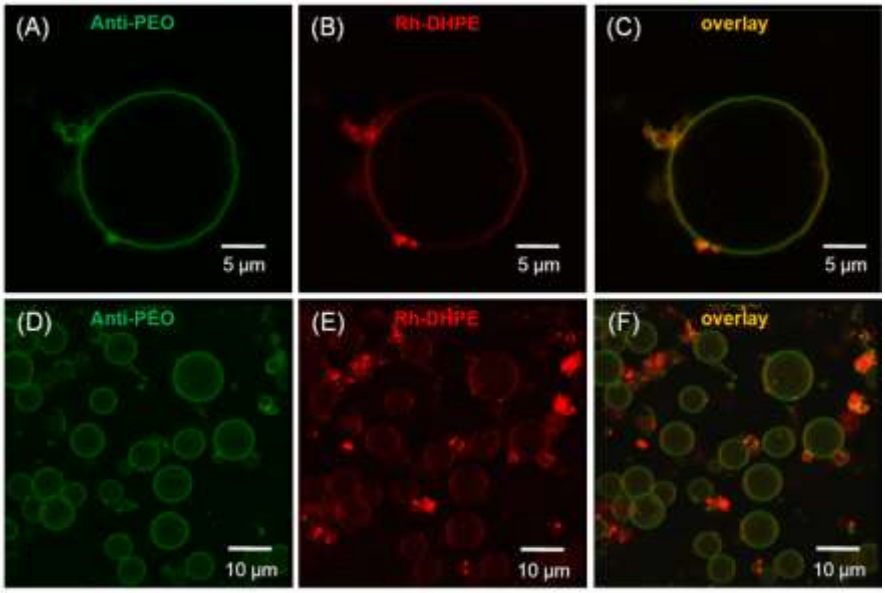

Figure S7. Confocal microscopy images of hybrid GUVs from a DOPC mixture with 20 mol% of BCP showing in (A to C) a single GUV image near the vesicle equator which display that the binding of the antibodies (excited at 488 nm, green) is uniformly observed over whole GUV surface. Panel (B) depicts the same vesicle using Rh-HPE (excited at 561 nm, red) to visualize the membrane morphology, which showed also a uniform distribution in the membrane. Panel (D-F) shows 3D-reconstruction of an axial series of confocal slices from an overview of hybrid GUVs, which displays the uniform fluorescence signal of the surface bond antibodies and Rh-DHPE for all vesicles proving the mixed state of the hybrid membrane. The obtained GUVs were stable over time (monitored over several hours) demonstrating no phase separation phenomena.

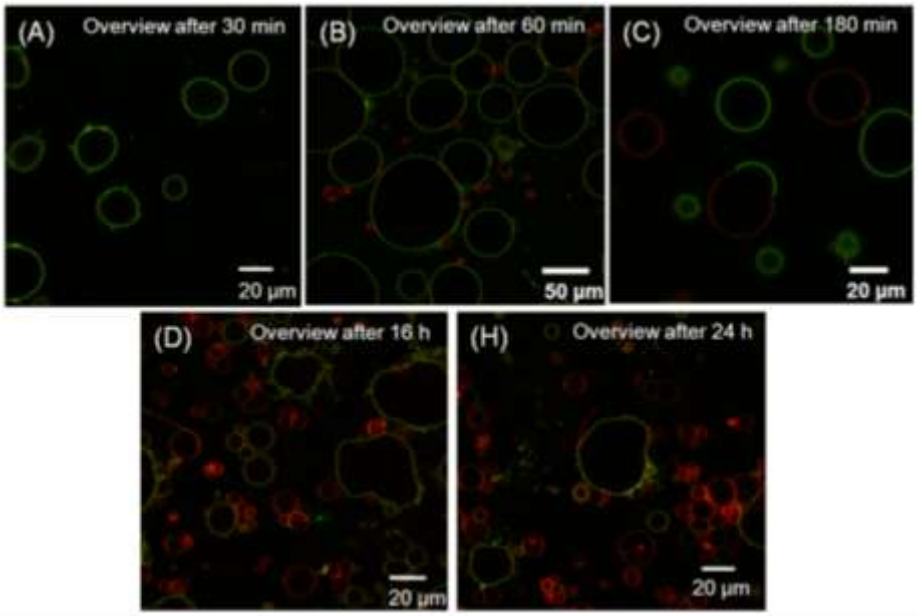

Figure S8. Selective antibody binding revealed that the hybrid vesicles prepared from mixtures of DOPC with 10 mol% of BCP and less polymer content undergo phase separation and a budding process with time. Panel (A to H) depicts confocal microscopy images (overlay image of antibody and Rh-HPE excitation) of hybrid GUVs, which were prepared from DOPC mixture with 10 mol% BCP, near their vesicle equator taken from different vesicles over time. Initially stable GUVs (no red-colored GUVs) were monitored over 24 hours demonstrating the formation of pure DOPC liposomes with time (compare amount of red colored vesicles in overlay images, visualized by Rh-DHPE dye). The analysis of the hybrid vesicles at different times allowed the observation of the budding process proving that the amount of red-colored vesicles is significant increased with time proving that no antibody binds to these vesicles (compare green and red areas in overlay images).

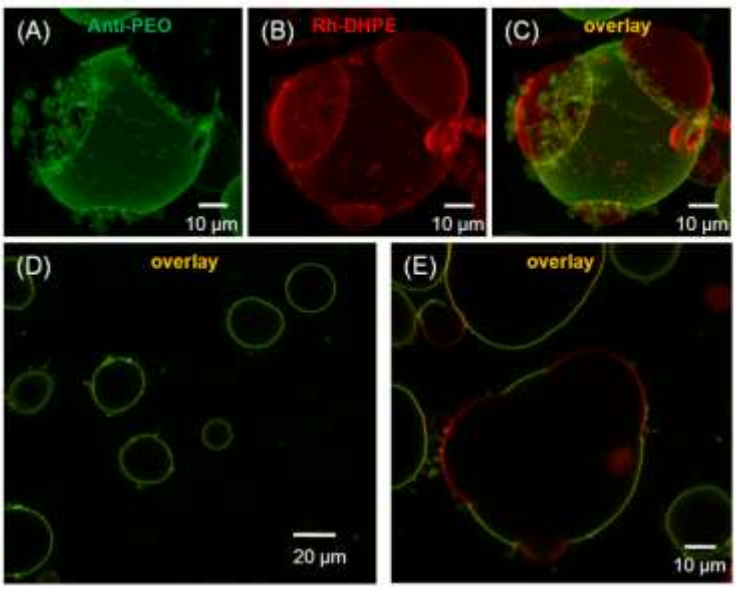

Figure S9. Selective antibody binding revealed that the hybrid vesicles obtained from 10 mol% BCP and less polymer content in mixtures with DOPC undergo phase separation and budding process with time. Panel (A-C) depicts a 3D-reconstruction of an axial series of confocal slices from a hybrid vesicle, which is shown in panel (E) as single slice near the vesicle equator, demonstrating the advanced state of the vesicle budding process (recorded at 85 minutes after secondary antibody incubation). Panel (A) displays the fluorescence signal of the surface bond antibodies (excited at 488 nm, green), panel (B) the fluorescence of the Rh-DHPE dye (excited at 561 nm, red) and panel (C) the overlay image indicating clearly that the vesicle undergoes budding, which results in the formation of polymer-depleted liposomes and polymer-rich vesicles. Panel (D) shows an overview image of hybrid GUVs after a short time after the electroformation process and antibody incubation, where no budding phenomena were observed expecting first stable GUVs.

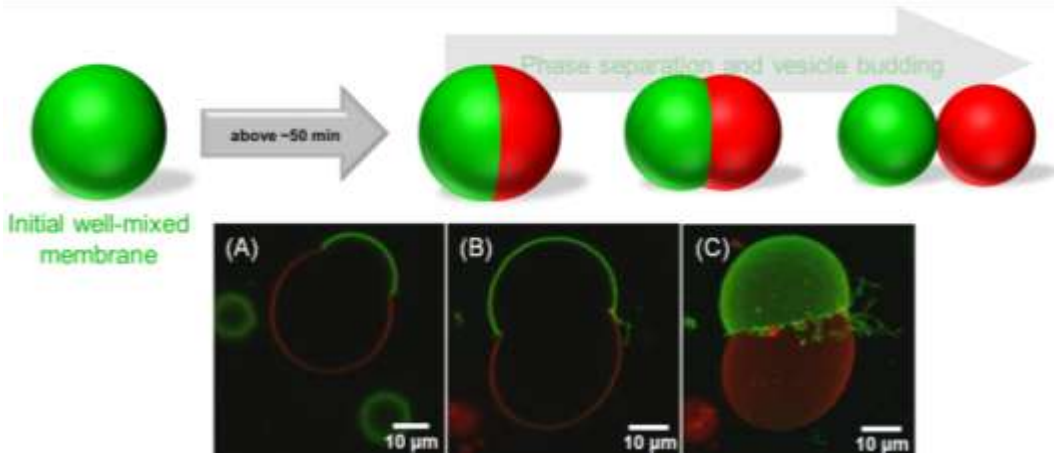

Figure S10. Schematic representation of the vesicle budding process compared to different states of the process obtained by fluorescence monitoring of different vesicles by LSM (panel A to C). During the budding the length of the domain boundary is strongly reduced which drives the vesicle fission process to completeness. Panel (A) shows a vesicle obtained form a mixture of DOPC with 10 mol% of BCP at an early state of the budding process, panel (B) at advanced state of the process and panel (C) depicts the 3D-reconstruction of the vesicle from (B) demonstrating clearly the coexistence of two different phases, the lipid-rich phase (visualized by Rh-DHPE, red area) and the polymer-rich phase (visualized by the fluorescently labeled antibodies, green area).

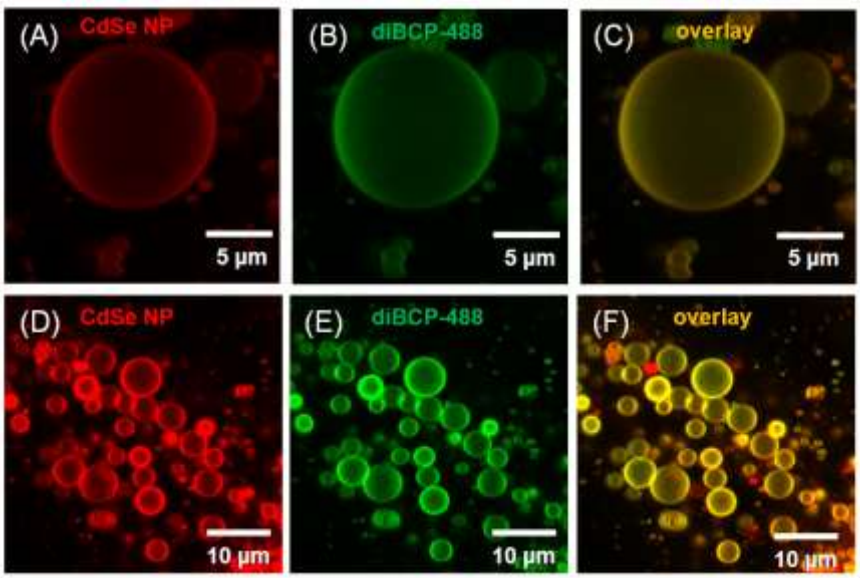

Figure S11. Incorporation of hydrophobically modified CdSe-NPs into DPPC/BCP hybrid membranes at room temperature is presented. (A to C) Confocal microscopy images of hybrid GUVs from a DPPC mixture with 18 mol% of BCP showing a single equatorial slice of a hybrid GUV which demonstrates that the CdSe-NPs (fluorescently labeled with rhodamine B; excited at 561 nm panel A) and the fluorescently labeled diBCP (excited at 488 nm, panel B) are randomly distributed within the hybrid bilayer proving the mixed membrane state. Panel (D-F) shows 3D-reconstruction of an axial series of confocal slices from an overview of hybrid GUVs, which displays the uniform fluorescence signal of the nanoparticles and labeled BCPs within the mixed bilayer in case of all vesicles proving further the mixed state of the hybrid membrane.

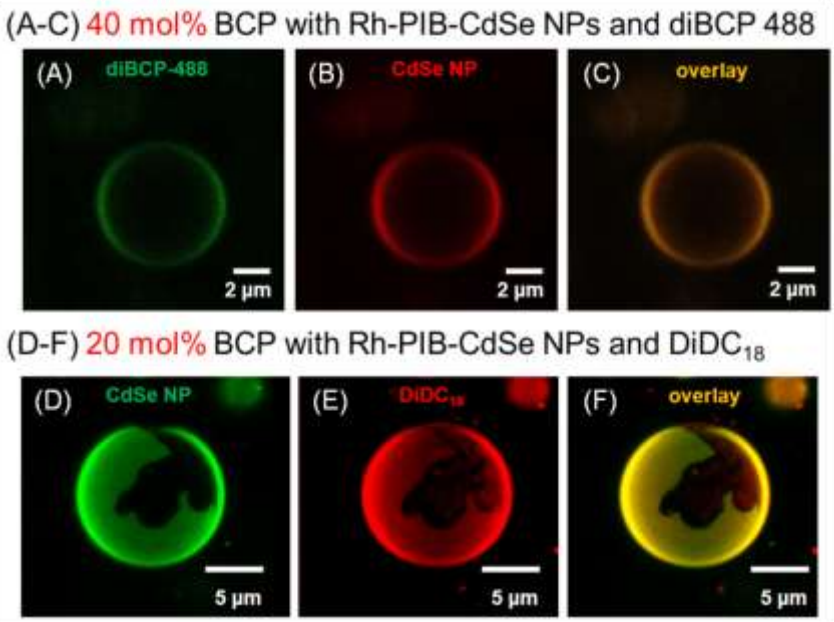

Figure S12. Incorporation of hydrophobically modified CdSe-NPs into DPPC/BCP hybrid membranes is demonstrated in the non-phase separated and phase separated case. The incorporation into mixed vesicles prepared from 60 mol% of DPPC and 40 mol% of BCP is shown in panel (A to C) and the selective localization of the particles in the polymer-rich phase of heterogeneous vesicle morphologies (obtained from mixtures of DPPC with 20 mol% BCP) is depicted in panel (D-F), which shows that the CdSe-NPs (excited at 561 nm) are preferential incorporated into one specific phase (green area in panel D). The enrichment of $DiDC_{18}$ used as additional membrane dye (panel E) indicates that the black patch in panel (D) consists of an ordered phase of DPPC molecules. The NP monitoring showed clearly that the particles prevent the incorporation into this ordered phase (see black patch in panel D and overlay image panel F).

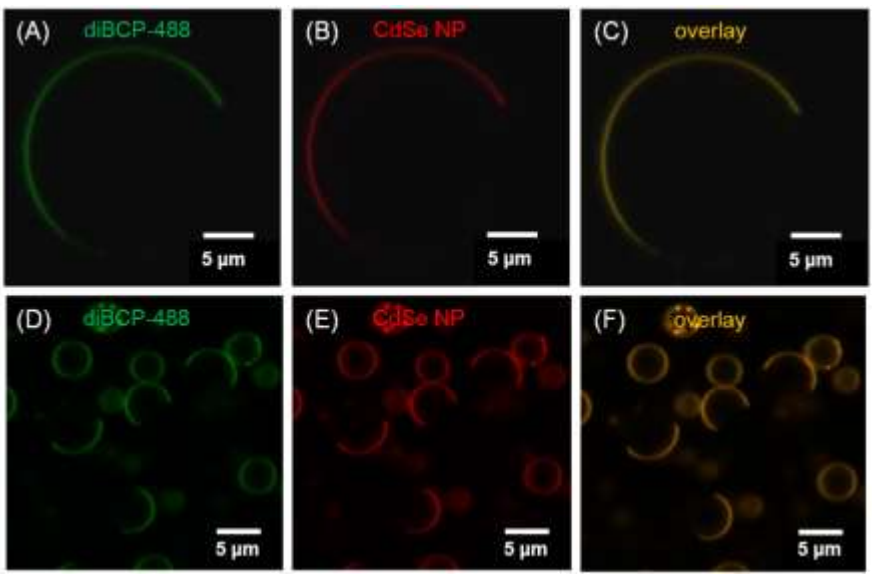

Figure S13. Selective incorporation of hydrophobically modified CdSe-NPs into DPPC/BCP hybrid membranes demonstrating the incorporation into the polymer-rich phase of heterogeneous vesicle morphologies (24 mol% BCP), which is confirmed by co-localization of the CdSe-NPs (fluorescently labeled with rhodamine B; excited at 561 nm panel B) and the fluorescently labeled diBCP (excited at 488 nm, panel A). (D to F) Confocal microscopy images of hybrid GUVs showing a single equatorial slice of the hybrid GUVs, prepared from mixtures of DPPC with 24 mol% of BCP, which demonstrates the formation of different phases and that the fluorescently labeled particles and block copolymers are partitioned into the same phase, preventing the incorporation into the observed black domains (ordered DPPC-rich phases).

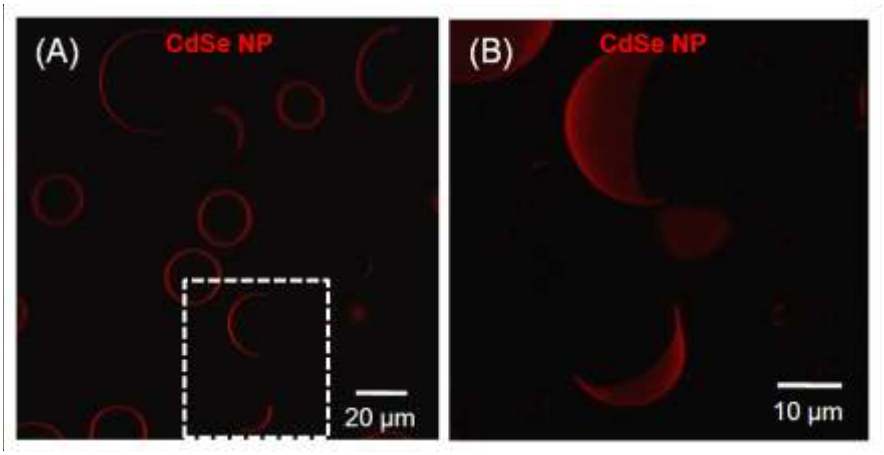

Figure S14. Confocal microscopy images of hybrid GUVs presenting the selective incorporation of hydrophobically modified CdSe-NPs into phase separated D**O**PC/BCP hybrid membranes (from mixtures of DOPC with 10 mol% BCP). The coexistence of two different phases is displayed by monitoring the fluorescently labeled nanoparticles (excited at 561 nm), which shows the preferential incorporation of the particles into one of the coexisting phases. Panel (A) depicts a single equatorial slice of hybrid GUVs and panel (B) illustrates a 3D-reconstruction of an axial series of confocal slices of hybrid GUVs (see indicted area in panel A) proving phase heterogeneities already obtained after electroformation process and before the GUVs were incubated with the antibody system.

References

1. Dyck, M.; Lösche, M., Interaction of the Neurotransmitter, Neuropeptide Y, with Phospholipid Membranes: Film Balance and Fluorescence Microscopy Studies *J. Phys. Chem. B* 2006, **110**, (44), 22143-22151.
2. Schulz, M.; Werner, S.; Bacia, K.; Binder, W. H., Controlling Molecular Recognition with Lipid/Polymer Domains in Vesicle Membranes. *Angew. Chem. Int. Ed.* 2013, **52**, (6), 1829-1833.
3. Korlach, J.; Schwille, P.; Webb, W. W.; Feigenson, G. W., Characterization of lipid bilayer phases by confocal microscopy and fluorescence correlation spectroscopy. *PNAS* 1999, **96**, (15), 8461-8466.